A Four-Channel Broadband MRI Receive Array Coil

Jue Hou, Courtney C. Bauer, Chenhao Sun, Ben Malone, Jay Griffin and Steven M. Wright, *Fellow, IEEE*

***Abstract*— Low-impedance preamplifier decoupling is commonly used in RF coil array construction to minimize coupling between elements through mutual impedance. The trap circuit is an essential component in preamp decoupling techniques, but becomes a limiting factor in constructing multi-tuned, multi-nuclear coil arrays. In principle, it is possible to double-tune or multi-tune the trap circuits, but will add complexity and loss. We present a broadband decoupling approach using high impedance preamplifiers. A dual-tuned prototype four-channel array using this approach which targets ^{2}H and ^{23}Na at 4.7T, has been previously constructed, evaluated and reported. Without any retuning of the array, the same setup is tested at the ^{23}Na and ^{31}P frequencies for 3T. Initial bench measurements and Chemical Shift Imaging (CSI) results are acquired and presented in this study.**

***Clinical Relevance*— This study could reduce the complexity of multi-nuclear array coil design.**

I. Introduction

RF coil array construction is complicated by mutual impedance between the coils, which changes the receive pattern of the elements. Many approaches provide decoupling, but by far the most common in receive arrays is to use what is known as 'preamplifier decoupling' [1]. Introduced by Roemer in his seminal paper on MR phased arrays, this technique uses a low-impedance preamplifier in combination with a trap circuit to present an open-circuit to the RF coil element while maintaining a 50-ohm (typically) impedance match to the preamplifier. This approach has become ubiquitous, as it provides the needed decoupling to allow the receiver coils to function as independent elements, giving distinct and predictable sensitivity patterns useful for parallel imaging and optimal SNR combination. Unlike relying on what is known as geometric decoupling, which generally only works for a very few number of coils, preamplifier decoupling has enabled scaling of the array elements, allowing very large numbers of elements to be used. The large numbers enable high acceleration factors when using parallel imaging methods [2-4].

Interests are growing in X-nuclear MRI and MRS studies due to the additional metabolic and chemical information. For example, ^{23}Na and ^{31}P are potentially useful in Duchenne Muscular Dystrophy (DMD) studies. It has been shown that ^{23}Na can be used to detect treatment response in DMD patients at early stages [5], and many biomarkers in ^{31}P spectroscopy can support muscle assessment in DMD studies [6,7]. Unlike ^{1}H imaging, X-nuclear imaging and spectroscopy is usually more time consuming due to the need for signal averaging. It is also not uncommon for an X-nuclear study to use multiple X-nuclei, which in most cases require coil change and patient repositioning, which further lengthens the overall study time. To reduce study time and complexity, it is of interest to develop double-tuned or multi-tuned coil arrays.

The significant limitation of the conventional approach to preamplifier decoupling, presenting a low-impedance to a trap circuit, is that it is narrow-banded. Most double tuning methods introduce a significant loss at one of the frequencies and a minor loss at the other. However, double tuning even the coil elements adds significant complexity to the array design. It is possible to double tune a conventional preamplifier design, at least in principle [8]. However, this adds a great deal of complexity, and may present a limiting factor in developing array coils for multinuclear applications.

Here we discuss a new approach to preamplifier decoupling that operates over a broad bandwidth. Rather than tuning a trap circuit, this method relies on using the high impedance of a preamplifier to provide inherent isolation. To ensure a good noise match, the input impedance of the RF coil is transformed through a wire-wound transformer. Both of these approaches are inherently broadbanded. We demonstrate broadband decoupling over a frequency range from 30.7 MHz to 52.9 MHz, and demonstrate the effectiveness of the approach by using a single four-channel array. To illustrate the broadband performance, bench S21 measurement using a dual-probe is done for the proposed array in comparison with standard 50-ohm tuned and matched coils. Imaging results have been collected for ^{2}H and ^{23}Na on a 4.7T scanner, and have been previously reported [9]. The same array is then tested with Chemical Shift Imaging (CSI) for ^{23}Na and ^{31}P on a 3T magnet, with no adjustment or retuning of any elements for either system or frequency.

II. Methods

A. Four-Channel Array Design

A four-channel circular array was initially built and tested at ^{23}Na, ^{2}H and ^{1}H in a 4.7T magnet. These frequencies were selected as they all allowed imaging in relatively short times,

*Research supported by National Institutes of Health through grant R01EB028533.

J. Hou is with the Department of Electrical and Computer Engineering, Texas A&M University, College Station, TX 77843 USA (e-mail: jzh93@tamu.edu).

C. C. Bauer is with the Department of Electrical and Computer Engineering, Texas A&M University, College Station, TX, 77843 USA. (e-mail: courtneybauer@tamu.edu).

B. Malone is with the Department of Electrical and Computer Engineering, Texas A&M University, College Station, TX, 77843 USA. (e-mail: texasmasadas3@tamu.edu).

C. Sun was with the Department of Electrical and Computer Engineering, Texas A&M University, College Station, TX, 77843 USA. (e-mail: chenhao.sun@yale.edu). Current address is Magnetic Resonance Research Center, Yale University, New Haven, CT 06511 USA.

J. Griffin is with the Department of Large Animal Clinical Sciences, Texas A&M University, College Station, TX 77843 USA (e-mail: jgriffin@cvm.tamu.edu).

S. M. Wright is with the Departments of Electrical and Computer Engineering and Biomedical Engineering, Texas A&M University, College Station, TX 77843 USA (e-mail: smwright@tamu.edu).

and there is significant interest in ^{2}H and ^{23}Na imaging [10-12]. Each element of the array is constructed with an 8 cm by 10 cm square loop using the proposed decoupling configuration. The imaging results at 4.7T have been previously reported and submitted as a journal paper [9]. Our group is also working on using ^{31}P spectroscopy and ^{23}Na imaging in a dog model for Duchenne Muscular Dystrophy. In this study we investigate whether the same coil used earlier at 4.7T could be directly applied to these new studies.

The four-channel array is double-tuned to the ^{2}H and ^{23}Na frequencies at 4.7T and is shown in Figure 1. An acrylic round tube with 4.5-inch diameter is used to support the array and hold the phantom. To demonstrate the decoupling performance of the proposed configuration, the array elements are overlapped to evenly cover a full circle, but not optimized for geometrical decoupling between adjacent elements. For ambient noise suppression on the cable shield, four dual-tuned cable baluns are built and tuned to the ^{2}H and ^{23}Na frequencies at 4.7T, and attached to the array.

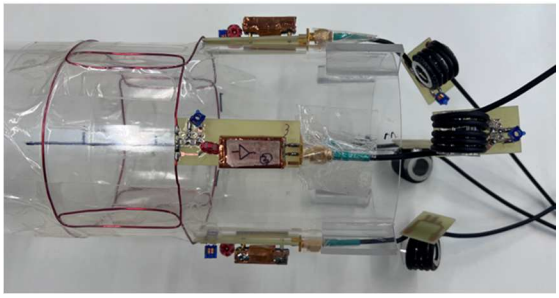

Figure 1. The four-channel coil array using the proposed high impedance preamplifier decoupling configuration.

B. *High Impedance Preamplifier Decoupling*

In the conventional preamplifier decoupling design, a low input impedance preamplifier and a narrow-band LC network together present a high impedance to the coil and 50-ohms to the preamplifier. Therefore, the coupling between coil elements can be suppressed by minimizing the current flow. This design is easy to achieve in a single-tuned array, but is complicated to extend to double-tuned or multi-tuned arrays. In this paper, we propose a different approach which uses a high impedance preamplifier to achieve the same goal. In this case, the coil element is tuned to resonant at the desired frequency, and the impedance is up-transformed to noise match the preamplifier. In the meantime, the high input impedance of the preamplifier is down-transformed by the transformer, but is still sufficiently high to provide coil decoupling. Unlike the traditional decoupling technique, this design in theory can provide broadband coil decoupling, as the high input impedance of the preamplifier and the transform ratio of an ideal transformer are independent of frequency.

To demonstrate the broadband performance of the proposed configuration, one element of the four-channel array is used for bench measurement. A standard double-tuning LCC network is used to serial resonant the coil at 30.7 MHz and 52.9 MHz frequencies, which are ^{2}H and ^{23}Na at 4.7T. Then, an air-core transformer with transform ratio of 1:3 is used for up-transforming the coil impedance and is connected to the preamplifier. A low noise high impedance amplifier (elcry1-u, Elcry Electronics, Denmark) is chosen in this study and is packaged with AC coupling capacitors and RF chokes as required by the manufacturer. For comparison, standard 50-ohm coils with the same dimensions are constructed at all frequencies of interest. Both matching and decoupling configurations are shown in Figure 2. By using a dual pick-up probe and a vector network analyzer in S21 mode, the resonance response of one coil in the array is evaluated over a broad bandwidth covering all frequencies of interest. Although the array is designed and tuned to operate at 30.7 MHz and 52.9 MHz, the comparison with S21 measurement is also done at 32.5 MHz and 49.8 MHz, which are the ^{23}Na and ^{31}P Larmor frequencies at 3T, respectively. No further tuning is done on the coil in order to demonstrate the flexibility and the broadband feature of the proposed decoupling approach.

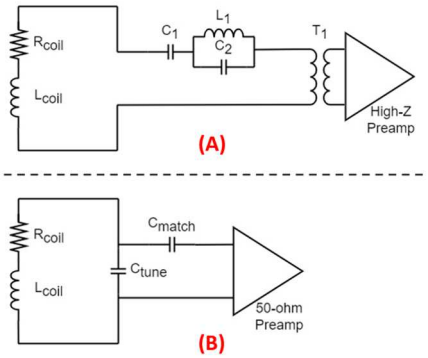

Figure 2. (A) The proposed high impedance matching and decoupling configuration. (B) The standard 50-ohm matching and tuning configuration used for the reference coil.

C. *Transmit Coil Design*

In order to transmit RF power at the frequencies of interest, a 6-inch-long saddle coil is constructed with ¾ inch wide copper tape on a 6-inch diameter acrylic tube. Active detuning with PIN diodes is implemented to the transmit coil to prevent coupling between the transmit coil and the receive array during signal reception. A solenoid balun is built and connected to the transmit coil to suppress current on the cable shield. The saddle coil is used for transmitting RF power at all frequencies of interest, and both the transmit coil and the balun can be easily retuned when switching the experiment frequency.

D. *Image Testing at 4.7T*

^{2}H and ^{23}Na imaging tests are performed on a Varian 4.7T scanner with an EVO spectrometer. Parallel imaging with the proposed four-channel array is performed at both frequencies separately, and a single-channel reference coil with conventional preamp decoupling is imaged for SNR comparison. A gradient echo pulse sequence with 100 ms TR and 4 ms TE is used for imaging at both frequencies. A 5-compartment phantom with various deuterium and NaCl concentrations is built with a 90 mm diameter cylindrical container. In addition, although not tuned to ^{1}H frequency, reference images were also acquired to show the capability of spatial localization using the array.

E. *CSI Testing at 3T*

In order to demonstrate the broadband performance and tuning flexibility of the proposed design, the same four-channel array is tested on a 3T SIEMENS Verio scanner with

a CSI FID pulse sequence for ^{23}Na (32.5 MHz) and ^{31}P (49.8 MHz) without any retuning. Direct gradient echo imaging was not available. The same saddle transmit coil along with its balun are used for transmitting RF power and are re-tuned to the Larmor frequencies of the experiments. A 5-compartment

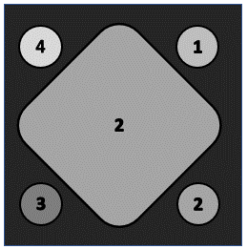

Vial	Concentration	Vial	Concentration
1	60mM 31P	3	20mM 31P
	150mM 23Na		50mM 23Na
2	40mM 31P	4	80mM 31P
	100mM 23Na		200mM 23Na

Figure 3. Transverse illustration image of the ^{23}Na and ^{31}P phantom used for the 3T CSI experiments. A gradient of ^{23}Na and ^{31}P concentration has been used and is shown in the table to the right.

^{23}Na and ^{31}P phantom is made with various NaH_2PO_4 and NaCl solution, as shown in Figure 3.

To connect the testing setup to the SIEMENS Verio scanner, an interface cable is constructed based on a standard SIEMENS 1TX/8RX connector for easy conversion between ODU cables and SMA/BNC connectors. The X1 connector on the patient table is used for utilizing an X-nuclei local transmit coil, and four of the eight receive channels are used to connect the four-channel array. Two of the PIN diode signal lines are used to tune or detune the transmit coil during scan. The interface cable enables us to easily switch between experiments, and provides flexibility for future coil development and testing. Shimming is not performed as the ^{1}H body coil is not selectable in the preliminary testing.

The CSI data is processed with MATLAB. Raw data files are exported from the SIEMENS system in ASCII format, and imported into MATLAB. The data processing included line broadening on all spectra, followed by zero-padding the matrix to 64x64 from 32x32 in the image direction. The array data was combined using the Sum-of-Squares approach. Due to the lack of shimming during the experiments, the images were reconstructed by integrating in the spectrum dimension over a range of 12 points, centered at the peak.

III. Results

A. Bench Measurement

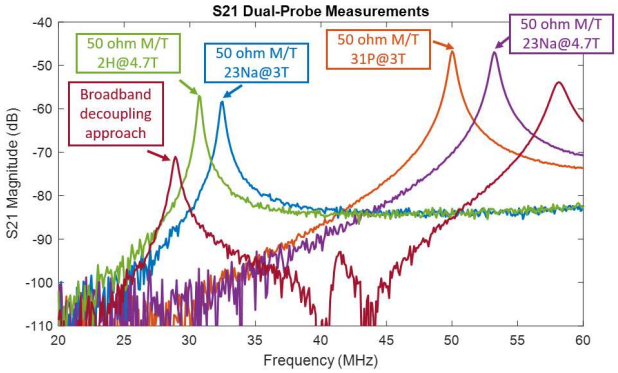

Figure 4. Bench S21 measurement using dual-probe of the proposed configuration versus the 50-ohm standard match/tune reference. Reference loop coils are tuned and matched to 50-ohm load at ^{2}H and ^{23}Na frequencies at 4.7 T, and ^{23}Na and ^{31}P frequencies at 3T.

To demonstrate the broadband feature of the proposed configuration, bench S21 measurement using a dual-probe are performed at the ^{2}H and ^{23}Na frequencies for 4.7T and at the ^{23}Na and ^{31}P frequencies for 3T. As shown in Figure 4, without any retuning of the decoupling network, the proposed configuration measures two resonance peaks that are outside of all the frequencies of interest. This measurement shows the

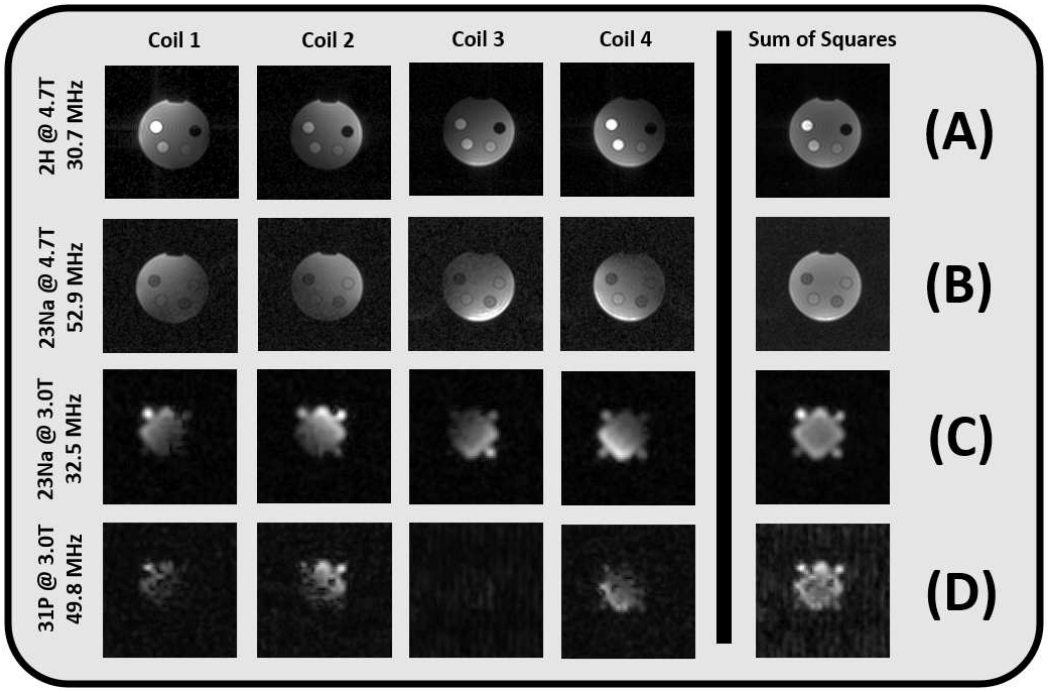

Figure 5. (A) and (B) are ^{2}H and ^{23}Na images acquired at 4.7 T using the four-channel array. (C) and (D) are ^{23}Na and ^{31}P CSI images acquired at 3T using the same array without any adjustment and retuning.

suppression of the induced current on the coil, which implies significant decoupling is provided over the wide bandwidth.

B. 4.7T Imaging Data

Imaging data is collected for the ^{2}H and ^{23}Na nuclei on a Varian 4.7T small animal magnet with a gradient echo sequence. Images from the individual coils are shown in Figure 5 (A) and (B). As surface receive elements acquire only within the region localized to the coil, a thresholding approach is developed to discriminate between signal and noise. As a means to accomplish this, a region is selected within the image, carefully avoiding test tubes as to only include the homogenous background region of the phantom. Within that region, a maximum value is found, and a threshold is set at 60% of that maximum value. The average SNR for the coils is found to be 169.8 for ^{2}H, and 46.05 for ^{23}Na. These are 76% and 89% of their respective references utilizing the conventional preamplifier decoupling configuration.

C. 3T CSI Data

The CSI_data is acquired on the Verio 3T scanner using the proposed array using a CSI FID pulse sequence. The same parameters are used for both ^{23}Na and ^{31}P experiments, with TR/TE = 540/2.3ms, slice thickness = 25 mm, FOV = 200x200 mm, and matrix size = 32x32. A total of 16 averages are performed for both nuclei for improved SNR. The images are reconstructed based on the CSI raw data and are shown for both the individual elements and the Sum-of-Squares reconstruction in Figure 5. The data demonstrates that the proposed array can successfully acquire images for ^{23}Na and ^{31}P at 3T without any retuning, and indicate no presence of coupling between elements. It is noticed that coil 3 shows mostly noise at the ^{31}P frequency, which could indicate a failed connection in the setup and is to be further investigated in the future. Although the preliminary CSI results do not serve as a thorough evaluation of the array performance, they do demonstrate the decoupling capability and highlight the broadband feature of this approach for multinuclear coil array development.

IV. Conclusion

In this study, we demonstrate the feasibility of broadband decoupling using a high impedance preamplifier and a transformer for multinuclear array coils. The ^{2}H and ^{23}Na imaging data acquired with the array at 4.7T shows good decoupling performance and acceptable SNR losses. Without any retuning and adjustment of the array, preliminary ^{23}Na and ^{31}P CSI data is acquired at 3T using the same array. Although lack of careful SNR comparison with another traditional coil array, the preliminary results do demonstrate the extreme simplicity and broadband decoupling potential of the array. It is promising that with further careful tuning and adjustment of the array, noise matching can be examined and improved, and the SNR performance can be optimized while maintaining broadband decoupling. In the future, instead of using the single LCC double-tuning network, which was only optimized for two frequencies, a single varactor diode can be used in each element as a DC controlled capacitor to better tune the element for noise matching to the preamplifier at the different frequencies. The approach demonstrated here has the potential to eliminate the need for nested arrays with multiple sets of decoupling preamplifiers, particularly in cases where some SNR loss may be acceptable.

References

[1] P. B. Roemer, W. A. Edelstein, C. E. Hayes, S. P. Souza, and O. M. Mueller, "The NMR phased array," *Magnetic Resonance in Medicine*, vol. 16, no. 2, pp. 192–225, Nov. 1990.

[2] D. K. Sodickson and W. J. Manning, "Simultaneous acquisition of spatial harmonics (SMASH): Fast imaging with radiofrequency coil arrays," *Magnetic Resonance in Medicine*, vol. 38, no. 4, pp. 591–603, Oct. 1997.

[3] M. A. Griswold, M. Blaimer, F. Breuer, R. M. Heidemann, M. Mueller, and P. M. Jakob, "Parallel magnetic resonance imaging using the GRAPPA operator formalism," *Magnetic Resonance in Medicine*, vol. 54, no. 6, pp. 1553–1556, Oct. 2005.

[4] S. M. Wright and L. L. Wald, "Theory and application of array coils in MR spectroscopy," *NMR in Biomedicine*, vol. 10, no. 8, pp. 394–410, Dec. 1997.

[5] M.-A. Weber et al., "Permanent muscular sodium overload and persistent muscle edema in Duchenne muscular dystrophy: a possible contributor of progressive muscle degeneration," *Journal of Neurology*, vol. 259, no. 11, pp. 2385–2392, Apr. 2012.

[6] D. P. Younkin, P. Berman, J. Sladky, C. Chee, W. Bank, and B. Chance, "31P NMR studies in Duchenne muscular dystrophy: Age - related metabolic changes," *Neurology*, vol. 37, no. 1, pp. 165–165, Jan. 1987.

[7] C. Wary, T. Naulet, J.-L. Thibaud, A. Monnet, S. Blot, and P. G. Carlier, "Splitting of Pi and other 31P NMR anomalies of skeletal muscle metabolites in canine muscular dystrophy," *NMR in Biomedicine*, vol. 25, no. 10, pp. 1160–1169, Feb. 2012.

[8] C.-H. Choi, S.-M. Hong, J. Felder, and N. J. Shah, "The state-of-the-art and emerging design approaches of double-tuned RF coils for X-nuclei, brain MR imaging and spectroscopy: A review," *Magnetic Resonance Imaging*, vol. 72, pp. 103–116, Oct. 2020.

[9] C. Sun, C. C. Bauer, J. Hou, and S. M. Wright, "Multinuclear receive coil array design using high impedance amplifiers for broadband decoupling," *Magnetic Resonance in Medicine*, submitted for publication.

[10] C. J. Eskey, A. P. Koretsky, M. M. Domach, and R. K. Jain, "2H-Nuclear Magnetic Resonance Imaging of Tumor Blood Flow: Spatial and Temporal Heterogeneity in a Tissue-isolated Mammary Adenocarcinoma1," *Cancer Research*, vol. 52, no. 21, pp. 6010–6019, Nov. 1992, Accessed: Feb. 07, 2023.

[11] H. M. De Feyter et al., "Deuterium metabolic imaging (DMI) for MRI-based 3D mapping of metabolism in vivo," *Science Advances*, vol. 4, no. 8, Aug. 2018.

[12] S. Konstandin and L. R. Schad, "30 years of sodium/X-nuclei magnetic resonance imaging," *Magnetic Resonance Materials in Physics, Biology and Medicine*, vol. 27, no. 1, pp. 1–4, Jan. 2014.